Acta Chemica Scandinavica, 1995: 49: 625–631
Printed in Belgium – all rights reserved

ACTA
CHEMICA SCANDINAVICA
ISSN 0904–213X

Structural Studies of a Particulate X-Ray Contrast Agent: A Multi-Method Approach

Lisbeth Ehnebom Tønnessen,[a] Rune Fossheim,[b] Jo Klaveness,[a] Berit Fjærtoft Pedersen[a,†] and Terje Thomassen[b]

[a]Institute of Pharmacy, University of Oslo, PO Box 1068, Blindern, N-0316 Oslo, Norway and [b]Nycomed Imaging AS, PO Box 4220, Torshov, N-0401 Oslo, Norway

Tønnessen, L. E., Fossheim, R., Klaveness, J., Pedersen, B. F. and Thomassen, T., 1995. Structural Studies of a Particulate X-Ray Contrast Agent: A Multi-Method Approach. – Acta Chem. Scand. 49: 625–631 © Acta Chemica Scandinavica 1995.

IEEC is a new X-ray liver contrast agent which has been studied by X-ray crystallography, NMR spectroscopy and molecular modelling. 1′-(Ethyloxycarbonyloxy)-ethyl-5-acetylamino-3(*N*-methylacetylamino)-2,4,6-triiodobenzene carboxylate, IEEC, $C_{17}H_{19}I_3N_2O_7$, $M_w = 744.06$ g mol^{-1}, crystallizes in the orthorhombic space group $P2_12_12_1$, $Z = 4$ with unit-cell dimensions $a = 10.489(3)$, $b = 11.677(6)$, $c = 19.466(6)$ Å and $V = 2384(1)$ Å^3. $R = 0.051$ for 2278 unique reflections. A head-to-tail intermolecular hydrogen bond N–H···O of 2.91(2) Å in the crystal structure gives the double ester side-chain an extended conformation. The structure is disordered, with two orientations of the *N*-methylacetanilido residue. The coexistence of 12 rotational isomers due to hindered rotations around the Ph–CO, Ph–N and N–CO bonds has been established by means of ^{1}H-NMR. The isomer composition obtained from NMR is in good agreement with the composition obtained from calculated molecular-mechanical energies for the same isomers. The two isomers found in the crystal structure are among the four most abundant isomers. Molecular-dynamics simulations and molecular-mechanics calculations suggest substantial flexibility in the double ester side-chain. In the calculated lowest-energy structure the ester chain is *pseudo*-normal to the ring as opposed to the extended conformation found in the crystal structure. The energy difference between these two conformations is 7.1 kJ mol^{-1}.

X-Ray contrast agents available today for medical diagnosis are hydrophilic water-soluble derivatives of benzene containing at least three iodine atoms. During the last decade there has been an increase in use of non-ionic agents (**1**) compared to ionic substances (**2**), due to the reduced osmolality, reduced toxicity and improved safety of the non-ionic agents.[1]

However, from an efficacy point of view, these agents all have very similar properties, showing the same pharmacokinetic profile; extracellular distribution and renal elimination.[2] Although magnetic resonance imaging (MRI) is now an established method in medical imaging with a large diagnostic potential, there is also a medical need for organ- and tissue-specific X-ray contrast agents, for example in the examination of the liver.

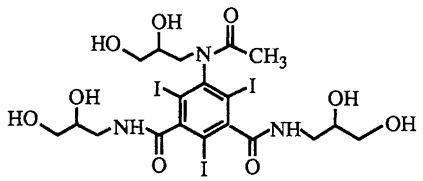

(**1**) iohexol

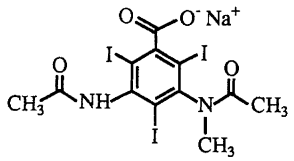

(**2**) sodium metrizoate

Intravascular particles in the micrometre range are rapidly taken up by cells in the liver, and various approaches for particulate liver X-ray contrast agents such as iodinated fat emulsions,[3] liposome encapsulated X-ray contrast agents[4] and various iodinated solid particles[5] have been evaluated.

1′-(Ethyloxycarbonyloxy)-ethyl-5-acetylamino-3(*N*-methylacetylamino)-2,4,6-triiodobenzene carboxylate

† To whom correspondence should be addressed.

(IEEC) (**3**) is a biodegradable water-insoluble (particulate) derivative of metrizoic acid (**2**) for X-ray liver imaging.[6–8] The double ester moiety in IEEC, which ensures effective enzymatic degradation by unspecific esterases and elimination of the particles *in vivo*, is of the same type as in, for example, some prodrug derivatives of penicillins, such as pivampicillin.

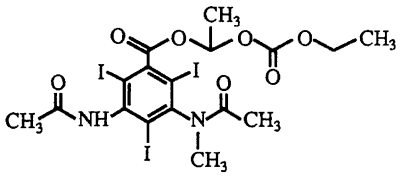

(**3**) IEEC

However, minor modifications in the double ester moiety of similar compounds have a large effect on the ability of the enzyme to degrade and dissolve the particulate product. The aim of this study has therefore been to analyze structural aspects of IEEC in order to gain a better understanding of the relationship between chemical structure and enzymatic degradation of iodinated particles in biological systems.

Experimental

X-Ray crystallography. Crystals suitable for X-ray investigation were obtained from a dimethyl sulfoxide (DMSO) solution by slow evaporation at room temperature. Data collection was performed at low temperature on a Nicolet *P3/F* automatic diffractometer with the ω–2Θ scan technique. The settings of 25 general reflections were used in a least-squares fit to determine the unit-cell parameters, $20 < 2\Theta < 30°$. The intensity data were corrected for Lorentz and polarization effects, and an absorption correction was applied by use of the program DIFABS.[9] Further details concerning crystallographic data and experimental conditions are summarized in Table 1.

Table 1. Crystal data and intensity collection.

Formula	$C_{17}H_{19}I_3N_2O_7$
Formula weight/g mol^{-1}	744.06
Crystal dimensions/mm^3	0.25×0.20×0.05
Density calculated/Mg m^{-3}	2.07
Linear absorption coefficient, μ/cm^{-1}	39.25
F(000)	1400
Space group	$P2_12_12_1$ (No. 19)
Z	4
a/Å	10.489(3)
b/Å	11.677(6)
c/Å	19.466(6)
V/Å^3	2384(1)
Diffractometer	Nicolet P3/F
Radiation	Mo*K*α
Wavelength/Å	0.710 69
Monochromator	Graphite
Temperature/K	138
Scan mode	ω–2θ
Scan range/°	$2\theta\alpha_1 - 1.0$ to $2\theta\alpha_2 + 1.2$
Scan speed/°min^{-1}	2
2θ range/°	3.0–60.0
Background/scan ratio	0.7
No. of reflections measured	5592
No. of unique reflections [$I > 3\sigma(I)$]	2278
Stability monitoring	3 test refl./ 135 observ.
$R = \Sigma \lvert \lvert F_o \rvert - \lvert F_c \rvert \rvert / \Sigma \lvert F_o \rvert$	0.051
$R_w = [\Sigma[w(\lvert F_o \rvert - \lvert F_c \rvert)^2] / \Sigma[w \lvert F_o \rvert^2]]^{1/2}$	0.057
$S = [\Sigma[w(\lvert F_o \rvert - \lvert F_c \rvert)^2] / (n-p)]^{1/2}$	4.58

Structure determination and refinement. The structure was solved by direct methods (MITHRIL),[10] which gave the atomic coordinates of the three iodine atoms. From a Fourier synthesis based on F_{obs}, 18 of the remaining 26 non-hydrogen atoms were located. Atoms in the *N*-methylacetanilido residue and the three outermost atoms in the double ester side-chain were missing. After several cycles of full-matrix least-squares refinement,[9] the missing non-hydrogen atoms were located by difference Fourier synthesis. All least-squares refinements were carried out by minimization of $\Sigma\, w\,(\Delta F)^2$, where $w = 1$. At this stage, the intensity data were corrected for absorption, and anisotropic thermal vibrations were included for the iodine atoms.

Further least-squares refinement showed irregularities in the geometry of the *N*-methylacetanilido residue, with bond distances of O2–C10 = 1.95, N2–C3 = 1.68, N2–C9 = 1.76, N2–C10 = 1.16 and C10–C11 = 1.16 Å, respectively. The atoms also showed large displacement parameters, with *U*-values of O2 = 0.09, N2 = 0.08, C9 = 0.05, C10 = 0.19 and C11 = 0.06 Å^2. Difference Fourier synthesis showed remaining electron density around the residue, suggesting that the *N*-methylacetanilido residue is disordered. The position of an alternative orientation was then included. Least-squares refinement of the atomic coordinates and occupancy factors of the two sites of the orientations (named A and B), with fixed displacement parameters, indicated a 50–50 distribution. Further least-squares refinement with the occupancy factors set to 0.5 gave a model with sensible displacement parameters and geometry. Hydrogen atoms were included at positions calculated from known geometry, and included in the final structure-factor calculation. The final difference map gave maximum and minimum residual electron densities of $\pm$ 1.45 e Å^{-3}. Atomic scattering factors were taken from Ref. 11. Final fractional coordinates and equivalent displacement parameters are given in Table 2.

Determination of absolute configuration. The absolute configuration was determined by refinement of the parameter ETA, the coefficient of the imaginary component of the anomalous scattering factor, in the GX program.[9] A

Table 2. Final fractional atomic coordinates with e.s.d.s in parentheses and equivalent isotropic displacement parameters (in Å^2).

Atom	*x*	*y*	*z*	*U*/Å$^{2\,a}$
I1	0.8962(1)	0.9338(1)	0.42273(6)	0.0337(6)
I2	1.4672(1)	0.8739(1)	0.40410(8)	0.0537(8)
I3	1.2075(1)	1.2367(1)	0.23135(5)	0.0324(6)
O1	1.389(2)	0.960(1)	0.1967(8)	0.061(4)
O2A	1.186(2)	0.730(2)	0.536(1)	0.033(5)
O2B	1.186(3)	0.680(2)	0.510(1)	0.039(6)
O3	0.892(1)	1.119(1)	0.2652(6)	0.037(3)
O4	0.948(1)	1.229(1)	0.3568(5)	0.027(2)
O5	0.777(1)	1.323(1)	0.4020(6)	0.039(3)
O6	0.635(2)	1.195(1)	0.3562(8)	0.055(4)
O7	0.603(1)	1.285(1)	0.4559(7)	0.047(3)
N1	1.427(1)	1.072(1)	0.2909(7)	0.031(3)
N2A	1.168(3)	0.814(3)	0.436(1)	0.028(6)
N2B	1.184(3)	0.861(3)	0.465(2)	0.035(7)
C1	1.079(1)	1.074(1)	0.3328(8)	0.024(3)
C2	1.073(2)	0.986(2)	0.3814(9)	0.034(4)
C3	1.184(2)	0.930(2)	0.3988(9)	0.039(4)
C4	1.301(2)	0.954(2)	0.372(1)	0.045(5)
C5	1.310(2)	1.045(1)	0.3210(8)	0.028(3)
C6	1.196(2)	1.102(2)	0.3045(8)	0.030(4)
C7	1.461(2)	1.023(2)	0.230(1)	0.039(4)
C8	1.589(2)	1.055(2)	0.2036(9)	0.038(4)
C9A	1.148(2)	0.701(2)	0.393(1)	0.045(5)
C9B	1.203(2)	0.921(2)	0.538(1)	0.047(5)
C10A	1.182(4)	0.821(3)	0.505(2)	0.035(8)
C10B	1.177(3)	0.741(4)	0.455(2)	0.037(8)
C11A	1.203(2)	0.921(2)	0.538(1)	0.047(5)
C11B	1.148(2)	0.701(2)	0.393(1)	0.045(5)
C12	0.965(2)	1.138(2)	0.3124(9)	0.031(4)
C13	0.854(2)	1.316(2)	0.342(1)	0.038(4)
C14	0.923(2)	1.433(2)	0.337(1)	0.060(6)
C15	0.666(2)	1.260(2)	0.4022(8)	0.031(4)
C16	0.479(2)	1.227(2)	0.465(1)	0.057(6)
C17	0.374(2)	1.291(2)	0.430(1)	0.067(7)

[a] $U_{eq} = 1/3\,\Sigma_i\Sigma_j \cdot U_{ij} \cdot \boldsymbol{a}_i^* \cdot \boldsymbol{a}_j^* \cdot \boldsymbol{a}_i \cdot \boldsymbol{a}_j$ (iodine atoms), U_{iso}, remaining atoms.

change in the sign of ETA during refinement indicated the opposite configuration to the one chosen, and hence the model was inverted.

NMR spectroscopic studies. The NMR spectra were recorded on a Varian VXR-300S spectrometer equipped with a 5 mm switchable broadband probe. The measurements were made at 298 K with DMSO-d_6 as solvent and 1% v/v TMS as internal reference.

Molecular modelling. In order to investigate the conformational flexibility of IEEC, molecular-dynamics simulations and molecular-mechanics calculations were performed. The crystal structure (with the A orientation of the *N*-methylacetanilido residue) was imported to the molecular graphics program INSIGHTII 2.3.0.[12] The molecule was energy-minimized from the crystal conformation using DISCOVER 2.95[12] with the CFF91 force field. Library charges supplied with this force field were used. The molecule was then subjected to a molecular-dynamics simulation at 600 K. This simulation lasted for 60 ps, after a 6 ps equilibration period. Coordinates observed every second ps were energy-minimized and written to disc, thus producing a total of 30 energy-minimized coordinate sets.

There are 16 isomers of IEEC that may arise as a result of hindered rotations around the Ph–CO, Ph–N and N–CO bonds. In order to investigate their stability they were first built from the lowest-energy structure obtained above by interactive rotations of the appropriate bonds. The resulting starting structures were then energy-minimized using DISCOVER.

All calculations were performed with a distance-dependent dielectric function ($\varepsilon = r_{ij}$) and torsion constraints imposed on the X–C(Ph)–C(Ph)–X torsion angles (force constant 2092 kJ Å^{-2}, value 0°). The step length for the dynamics simulations was 1 fs, and the convergence criterion for the energy minimizations was 0.13 kJ Å^{-2} using the BFGS (Broydon–Fletcher–Goldfarb–Shanno) minimization technique. All calculations were performed on a Silicon Graphics 4D/35 workstation running under the IRIX 4.0.5 operating system.

Results and discussion

The values of the bond lengths and angles from the X-ray structure determination are listed in Table 3. Since their estimated standard deviations are high, the geometry will not be discussed in detail. Figure 1 is an ORTEP[9] drawing of the molecule. For clarity only one orientation of the disordered *N*-methylacetanilido residue is given (orientation A). The two orientations of the residue (A and B) are illustrated in Fig. 2; both orientations have the methyl groups in the favourable *anti* position. The atomic sites of the methyl groups are interchanged, which means that C9 for one orientation occupy the same position as C11 for the other orientation. They are given the same atomic coordinates and displacement parameters, and an occupancy factor of 0.5 each (C9A = C11B and C11A = C9B). The two orientations are fairly well separated, the distance between N2A and N2B in the refined model being 0.81 Å, between O2A and O2B 0.78 Å and between C10A and C10B 1.35 Å, making refinement of separate positional parameters possible.

There is also disorder in the crystal structure of iopamidol,[13] which is the only other triiodinated contrast agent whose X-ray structure has been reported.

Packing pattern, intermolecular hydrogen bonding. The packing pattern in the crystal is shown in Fig. 3 (PLUTO).[14] There are no intramolecular, and only one intermolecular hydrogen bond. This occurs between one amide nitrogen atom (N1) and the carbonyl oxygen atom in the carbonate ester group (O6). The geometry of this N–H···O hydrogen bond is N1···O6 = 2.91(2) Å, N1–HN1···O6 = 1.86 Å and the angle N1–HN1···O6 is 162.1°. This head-to-tail hydrogen bond stabilizes an extended conformation of the molecule.

Table 3. Interatomic distances (in Å) and angles (in °), with e.s.d.s in parentheses.

C_{arom}–I	2.10(4)[a]	3[b]	C_{sp^3}–O_{ester}	1.45(5)	3
C_{sp^2}–O_{ester}	1.34(5)	3	C=O_{ester}	1.22(4)	2
C=O_{amide}	1.25(8)	3	N_{amide}–C_{sp^3}	1.59(6)	2
N_{amide}–C_{amide}	1.38(8)	3	N_{amide}–C_{arom}	1.48(6)	3
C_{sp^3}–C_{sp^3}	1.52(6)	2	C_{amide}–C_{sp^3}	1.39(8)	3
C_{arom}–C_{arom}	1.40(7)	6	C1–C12	1.47(3)	
I–C_{arom}–C_{arom}	120(3)	6	O_{ester}–C_{sp^3}–C_{sp^3}	108(3)	3
C_{sp^2}–O_{ester}–C_{sp^3}	118(2)	3	O_{ester}–C_{sp^2}=O_{ester}	124(3)	3
O3–C12–C1	128(2)		O4–C12–C1	109(1)	
O4–C13–O5	106(2)		O5–C15–O7	109(2)	
O=C_{amide}–N_{amide}	118(5)	3	O=C_{amide}–C_{sp^3}	122(5)	3
N_{amide}–C_{amide}–C_{sp^3}	119(5)	3	C_{sp^3}–N_{amide}–C_{amide}	126(4)	2
C_{sp^3}–N_{amide}–C_{arom}	121(3)	2	C_{amide}–N_{amide}–C_{arom}	116(5)	3
N_{amide}–C_{arom}–C_{arom}	118(5)	6	C_{sp^2}–C_{arom}–C_{arom}	121(3)	2
C_{arom}–C_{arom}–C_{arom}	120(5)	6			

[a] Mean value, mean value of e.s.d. calculated from $(\text{e.s.d.}_1^2+\text{e.s.d.}_2^2+\text{e.s.d.}_3^2+\cdots)^{1/2}$. [b] Number of observations.

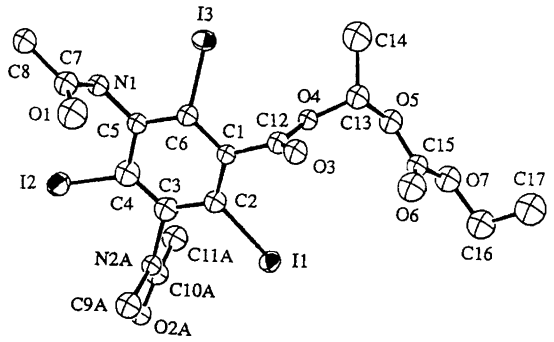

Fig. 1. Perspective drawing of the molecule.

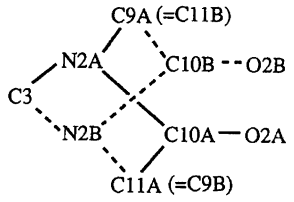

Fig. 2. The two orientations of the disordered *N*-methylacetanilido residue. Orientation B is shown by dotted lines.

There is one short intermolecular I···I contact of 3.93 Å and the crystal structure also shows short I···O contacts, 2.84–3.03 Å, from I1 and I2 to O2 (A and B). Such short I···I and I···O contacts are also observed in the structure of iopamidol[13] and for many thyroid-hormone structures.[15] There are three short C···O intermolecular contacts; the distances are given in Table 4 together with the other intermolecular short contacts.

Isomerism. The terminology that has been adopted for the possible rotational isomers of IEEC is as follows. The *exo* conformer is characterized by the carbonyl moiety of the acetanilido group pointing away from the aromatic ring, whereas the group is pointing towards the ring in the *endo* conformation. The different orientations of the ester chain relative to the acetanilido groups are described as *cis* when the carbonyl groups are on the same side of the ring and as *trans* when they are on opposite sides. Naming the *N*-methylacetanilido group first the following conformers are possible: *cis–cis*, *cis–trans*, *trans–cis* and *trans–trans*. The first and the last of these conformers imply a *cis* relationship between the acetanilido groups, whereas the other two imply a *trans* relationship. Combined with the *exo/endo* isomerism, this results in 16 distinct conformers.

The interconversion of rotational isomers in iodinated X-ray contrast agents is, in general, found to be slow on the NMR timescale at ambient temperatures. Accordingly, each rotamer displays a distinct and unique set of resonances in ^{1}H-NMR. Of the 16 possible isomers, the coexistence of 12 rotational isomers of IEEC in a solution of DMSO-d_6 at 298 K has been established by means of ^{1}H-NMR. Figure 4 shows the ^{1}H-NMR spectrum of IEEC together with an expansion of the CO–NH region, where the amide resonances are assigned in accordance with the results of molecular modelling and NMR results

Table 4. Intermolecular close contacts (in Å), with e.s.d.s in parentheses.

I1···I3[a]	3.934(2)	I1···O2A[b]	3.03(3)
I1···O2B[b]	2.89(3)	I2···O2A[c]	2.84(2)
I2···O2B[c]	2.92(3)	O1···C13[d]	3.14(3)
O3···C9A(=C11B)[a]	3.25(2)	O5···C11A(=C9B)[e]	3.30(3)
N1···O6[f]	2.91(2)		

Symmetry code: [a] $2-x$, $1/2+y$, $1/2-z$; [b] $x-1/2$, $3/2-y$, $1-z$; [c] $1/2+x$, $3/2-y$, $1-z$; [d] $2-x$, $y-1/2$, $1/2-z$; [e] $x-1/2$, $5/2-y$, $1-z$; [f] $x-1$, y, z.

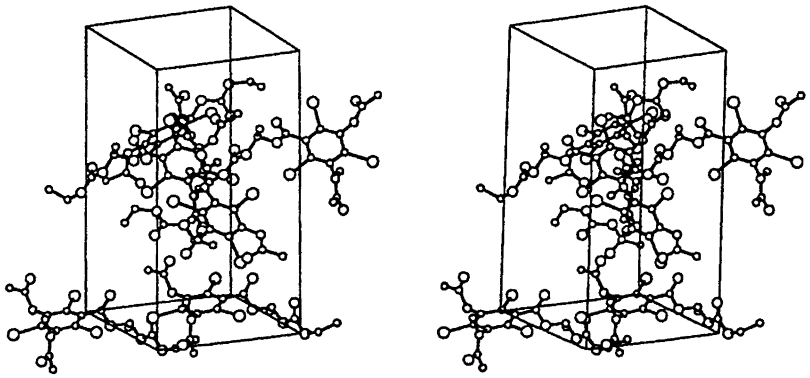

Fig. 3. Stereoscopic view showing the packing pattern of the molecule.

of simple model substances. The amide resonances fall into three groups of four resonances each. These resonance groups are assigned to the *exo–endo*, *endo–endo* and *exo–exo* conformers, where the *N*-methylacetanilido group is named first. The largest splitting of resonances in each of these groups is caused by a *cis/trans* relationship between the acetanilido groups. These resonances are then further split owing to a *cis/trans* relationship between the acetanilido and the ester residue.

The *N*-methylacetanilido residue prefers the *exo* conformation, while the secondary acetanilido residue prefers the *endo* conformation. After reaching a state of isomeric equilibrium the *exo–endo*, *endo–endo* and *exo–exo* ratio is found to be 83:14:3, respectively. The *endo–exo* isomer has not been detected by ^{1}H-NMR. These results are in excellent agreement with the populations obtained from the calculated conformational energies shown in Fig. 5. Using the Boltzmann distribution law for the 16 conform-

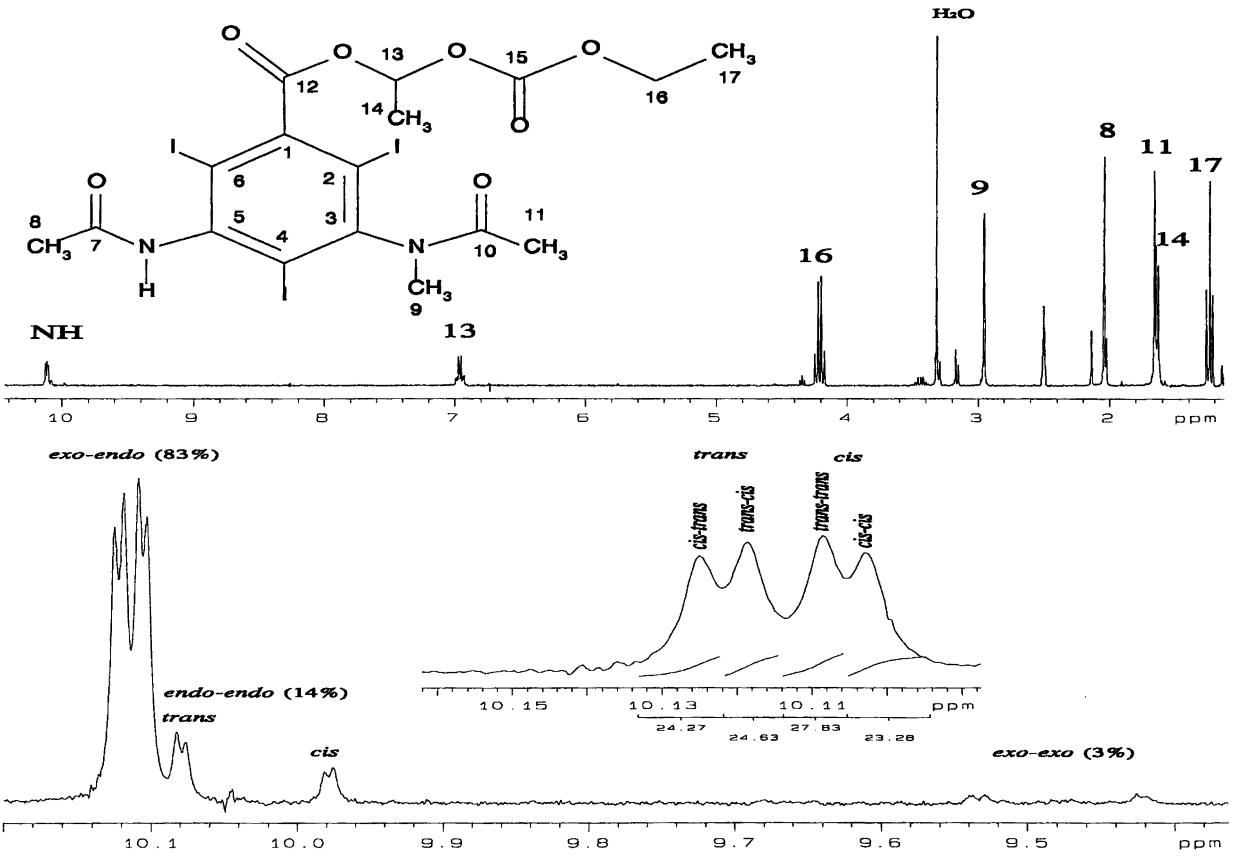

Fig. 4. ^{1}H-NMR spectrum of IEEC (only the major resonances and isomers are assigned). The assignment of *cis* and *trans* isomers is based on the results of molecular modelling.

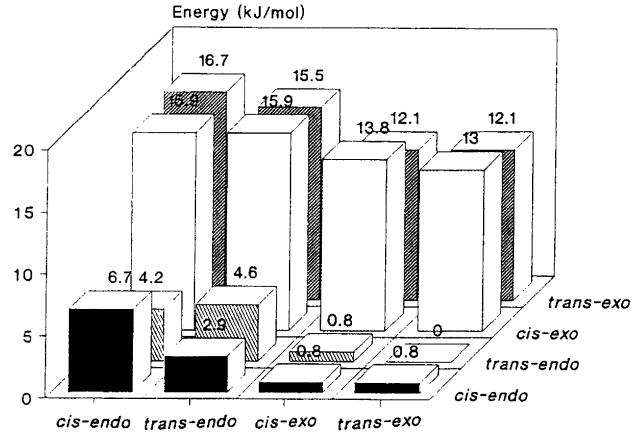

Fig. 5. Calculated conformational energies for IEEC. The *N*-methylacetanilido substituent is plotted along the *x*-axis and the *N*-H acetanilido substituent along the *y*-axis.

ers one obtains the partition function 3.87 and the conformer ratio 81:17:2 for the *exo–endo*, *endo–endo* and *exo–exo* isomers at 300 K. The energies for the *endo–exo* isomers are so high that they will be present only in minor amounts. In the crystal structure the molecule adopts the energetically favoured *exo–endo* conformation. The torsional angles indicating this are $-171(5)°$ (C3–N2A–C10A–O2A), $175(4)°$ (C3–N2B–C10B–O2B) and $5(2)°$ (C5–N1–C7–O1), respectively.

As for *cis/trans* isomerism, the NMR data suggest that the ratio of conformers in which the acetanilido carbonyl groups are on the same side of the ring (*cis–cis* and *trans–trans*) and on opposite sides (*cis–trans* and *trans–cis*) is dependent on the *exo/endo* isomerism in such a way that the ratio is 2:1 (or 1:2) for the *endo–endo* conformation and 1:1 for the *exo–endo* and *exo–exo* conformations. Whether *cis–cis/trans–trans* or *cis–trans/trans–cis* dominates in the *endo–endo* conformation could not be deduced from the NMR data. However, modelling results based on Boltzmann statistics suggest a ratio of 1:2, 1.2:1 and 1.3:1 for the *endo–endo*, *exo–endo* and *exo–exo* conformations, respectively. The low population of *cis–cis* and *trans–trans* in the *endo–endo* conformation can be explained by the fact that the negatively charged carbonyl oxygen atoms are brought in relatively close proximity when they are on the same side of the ring, and hence repel each other more than when they are on opposite sides of the ring. This effect is much less pronounced when the carbonyl groups are *exo*.

The modelling results suggest that the population of *cis–cis*, *trans–trans*, *cis–trans* and *trans–cis* will be 20:30:24:26, i.e. there will be a close to 1:1 ratio between the *cis–cis/trans–trans* and *cis–trans/trans–cis* conformers. The fact that the *endo–endo* isomer is not favourable for the *cis–cis/trans–trans* conformation does not influence the overall *cis–trans* equilibrium markedly, mainly because the *endo–endo* isomer constitutes only 14% of the isomeric mixture. The interpretation of NMR data (Fig. 4) and the results from molecular modelling are almost consistent regarding the *cis/trans* population ratios. The two conformations seen in the solid state are *trans–cis* (for the A orientation of the *N*-methylacetanilido residue) and *cis–cis* (for the B orientation). These conformers have the same energy. Since there is no steric hindrance for the occurrence of the two isomers in the crystal lattice, the gain in entropy will probably favour the existence of both.

No conclusions regarding the conformation of the ester chain can be obtained from the NMR data. The lowest-energy conformer obtained from the molecular-dynamics simulations and the molecular-mechanics calculations are shown superimposed on the crystal structure in Fig. 6 (upper part). It may be seen that the calculated structure differs from the conformation adopted in the solid state mainly in the orientation of the double ester side-chain. The double ester chain is *pseudo*-normal to the phenyl ring in the calculated structure, whereas it points away from the ring in the crystal structure with torsion angles pertaining to the double ester bond of 126.9 and $-95.4°$ in the crystal structure, and 156.6 and $-75.4°$ in the energy-minimized structure. These angles were enumer-

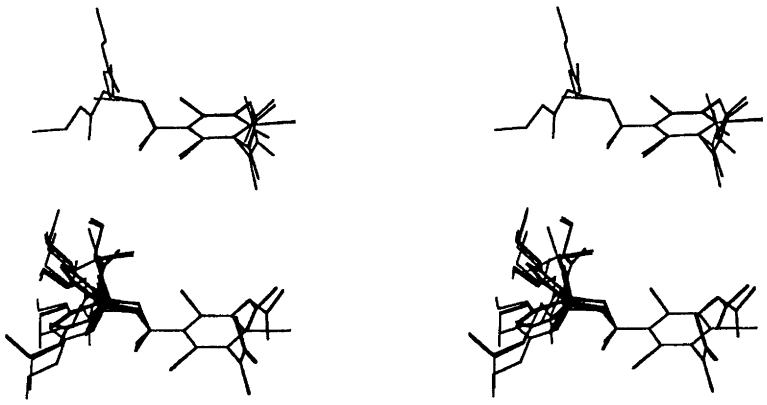

Fig. 6. Stereoview of the comparison between the computed lowest-energy conformer and the crystal structure (upper), superpositioning of the structures that are within 12.5 kJ mol^{-1} of the lowest-energy structure (lower).

ated outwards from the ring. This difference may be related to the more favourable packing energy of the extended conformation, which also incorporates an intermolecular hydrogen bond. However, the results of the calculations suggest that substantial flexibility is allowed in the double ester chain. Figure 6 (lower part) shows a superpositioning of the structures that are within 12.5 kJ mol^{-1} of the lowest-energy structure (the crystal structure is included in the superpositioning). It can be seen that quite different conformations are adopted, mainly caused by conformational flexibility in the CO–CHMe–OC part of the chain. The part of CO–CHMe–OC conformational space spanned by the low-energy structures comprise ($\pm$ *gauche/anti*, *anti*) and ($-$ *gauche/anti*, $-$ *gauche*) conformations, whereas ($\pm$ *gauche/anti*, $+$ *gauche*) and ($+$ *gauche*, $-$ *gauche*) are not adopted. The (+,+) and (−,−) conformers differ in energy in the present case owing to the chirality of the carbon atom in the double ester bond. It may be noted that steric strain distorts the *anti* conformations from their ideal values to ca. $\pm 150°$. The lowest-energy conformer adopting the same double ester conformation as found in the crystal structure is calculated to be 7.1 kJ mol^{-1} higher in energy than the lowest-energy structure.

Absolute configuration. The X-ray structure determination shows that the single chiral carbon atom in the molecule (C13) has the *S* configuration. The crystals were made from a racemic solution, which usually results in racemic crystals.[16] However, in certain cases separate crystallization of the enantiomers seems to be more favourable than the formation of racemic crystals. This was shown by Pasteur in his famous experiment sorting the single crystals of sodium ammonium tartrate by their exterior appearance. Selection of a different crystal for the X-ray data collection would therefore probably give the opposite absolute configuration.

Acknowledgement. We are indebted to Agnar Aasen, University of Oslo, Department of Chemistry, for assistance during the X-ray data collection.

References

1. Almén, T. *Am. J. Cardiol. 66* (1990) 2F.
2. Swanson, D. P., Chilton, H. M. and Thrall, J. H. *Pharmaceuticals in Medical Imaging*, MacMillan, New York 1990.
3. Ivancev, K., Lunderquist, A., Isaksson, A., Hochbergs, P. and Wretlind, A. *Acta Radiol. 30* (1989) 449.
4. Seltzer, S. E. *Radiology 171* (1989) 19.
5. Violante, M. R., Fischer, H. W. and Mahoney, J. A. *Invest. Radiol. 22* (1980) 329.
6. Gjøen, T., Holtz, E., Strande, P., Klaveness, J., Leander, P. and Berg, A. In: Ferrucci, J. T. and Stark, D. D., Eds., *Liver Imaging: Current Trends and New Techniques*, Chap. 45, Andover Medical Publishers Inc., Boston 1990.
7. Gjøen, T., Strande, P., Gołman, K., Klaveness, J., Leander, P. and Michelet, Å. A. *Invest. Radiol. 25S* (1990) 98.
8. Bjørsvik, H.-R. *Acta Chem. Scand. 48* (1994) 445.
9. Mallinson, P. R. and Muir, K. W. *J. Appl. Crystallogr. 18* (1985) 51.
10. Gilmore, C. J. *J. Appl. Crystallogr. 17* (1984) 42.
11. *International Tables for X-ray Crystallography*, Vol. 4, Kynoch Press, Birmingham 1974.
12. BIOSYM Technologies, Inc., 10065 Barnes Canyon Rd., San Diego, CA 92121.
13. Ganazzoli, F., Albinati, A. and Pitrè, D. *Acta Crystallogr., Sect. C 39* (1983) 1570.
14. Motherwell, W. D. S. *PLUTO*, University of Cambridge, Cambridge, UK 1976.
15. Cody, V. *Endocr. Rev. 1* (1980) 140.
16. Gilli, G. In: Giacovazzo, C., Ed., *Fundamentals of Crystallography*, Chap. 7, Oxford University Press, London 1992.

Received November 14, 1994.